Earthquake Geotechnical Engineering for Protection and Development of Environment and Constructions – Silvestri & Moraci (Eds)
© 2019 Associazione Geotecnica Italiana, Rome, Italy, ISBN 978-0-367-14328-2

Spatial distribution of landslides triggered by the 2016 Central Italy seismic sequence

E. Ausilio
Department of Civil Engineering, University of Calabria, Rende (CS), Italy

F. Silvestri
Department of Civil, Architectural and Environmental Engineering, University of Naples Federico II, Naples, Italy

G. Tropeano
Department of Civil Environmental Engineering and Architecture, University of Cagliari, Cagliari, Italy

P. Zimmaro
Department of Civil and Environmental Engineering, University of California, Los Angeles, CA, USA

ABSTRACT: Between August and October 2016, the Central Italy area, along the Apennine chain, has undergone a seismic sequence with three major earthquake events. The first event, with moment magnitude **M**6.1, occurred on 24 August 2016, the second (**M**5.9) on 26 October, and the third (**M**6.5) on 30 October 2016. Each event triggered a substantial number of coseismic landslides. The large majority of them are rock falls. For each mainshock, we analyze the spatial distribution of observed earthquake-induced landslides. Our analysis shows that data from this earthquake sequence are in good agreement with empirical relationships reported in the literature. We correlate the outermost landslide limits with peak ground acceleration (PGA) and peak ground velocity (PGV) spatial distributions, evaluated applying Kriging of within-event residuals. Values of PGA at the landslide limits for this seismic sequence are comparable to those observed during other earthquakes of comparable magnitude.

1 INTRODUCTION

In recent years, the spatial distributions of landslides triggered by earthquakes has been a widely studied problem. Most studies focused on examining the limit distances within which landslides have been observed during seismic events. Landslides limit distances depend on several factors such as geo-morphological, hydrological, and seismic conditions. Pre-event forecast of such limits is a useful tool to define areas that may be interested by seismically-induced landslides following future earthquakes.

Earthquake-induced landslide hazard is very significant in Italy. This is due to the combination of two factors: (1) seismic hazard in Italy is very high due to the presence of active shallow crustal and deep seismogenic sources, and (2) many Italian areas are prone to landslides. As a result, large earthquakes in Italy often trigger a relevant number of landslides (e.g. Govi, 1977; Del Gaudio and Wasowski, 2004).

Between 24 August 2016 and 30 October 2016, a wide region in Central Italy (a highly seismic area) was struck by several earthquakes. The 2016 Central Italy seismic sequence was characterized by three major earthquake events. The first event, with moment magnitude **M**6.1, occurred on 24 August 2016, the second (**M**5.9) on 26 October, and the third (**M**6.5) on 30 October 2016. Each event was followed by numerous aftershocks. All mainshocks were caused by normal faults part of the Mt. Vettore-Mt. Bove fault system. Several landslides and rockfalls were triggered by the seismic sequence (e.g. Romeo et al., 2017; Franke et al., 2018).

In this paper we analyze landslide types and their spatial distribution following all three mainshocks of the 2016 Central Italy earthquake sequence. Landslide types are classified following the commonly-used seismic landslide classifications proposed by Keefer (1984). We use the term *landslides* to define ground failure phenomena involving lateral and/or downslope movement of soil and/or rock. Such definition is consistent with that adopted by Keefer (1984). Landslides data are compared with empirical upper bound curves proposed by Keefer (1984) in terms of surface-wave magnitude (M_S) versus epicentral distance, envelope area affected by landslides, and distance from the fault-rupture zone. In this study, we characterize the distance from the fault-rupture zone using the well-known distance from the surface projection of the rupture surface (i.e. Joyner and Boore distance; R_{JB}) as preferred metric. We also compare magnitude-distance distribution of earthquake-induced landslides triggered during the 2016 Central Italy earthquake sequence with those observed following the **M**6.1 1997 Umbria-Marche earthquake. Finally, we show peak ground acceleration and velocity (PGA and PGV, respectively) distributions at the landslides limits. We anticipate that the availability of such high-quality data can be used to improve existing empirical relationships and microzonation studies (e.g. Silvestri et al., 2016).

2 RECENT ITALIAN CASE HISTORIES

In the last century, several seismic events in Italy have triggered a relevant number of landslides. The 1976 Friuli (Northern Italy) earthquake sequence was characterized by two mainshocks. The first mainshock occurred on 6 May with moment magnitude **M**6.4, while the second one on 15 September with moment magnitude **M**5.9. Both events, triggered almost entirely rockfalls and occurred near the tops of the rock-walled slopes. Most of these landslides were concentrated in the epicentral areas of both events. Ambraseys (1976) and Govi (1977) observed that the surface of rupture of some landslides coincided with pre-existing fracture planes.

During the **M**6.9 1980 Irpinia (Southern Italy) earthquake, the majority of earthquake-induced landslides were rock falls (47.2%). Translational and rotational slides were also numerous (40.2%) and occurred in areas characterized by highly susceptible lithological and morphological conditions (Esposito et al., 1998). A peculiar feature of landslides triggered by the Irpinia earthquake is represented by the delayed effects. Several instability phenomena (~24% of the total) occurred after several hours from the earthquake (Esposito et al., 1998). The time delay was up to 72 hours for some landslides. Such delayed responses were due to the fact that the materials involved in these landslides were saturated high-plasticity variegated, varicolored clays (Cotecchia and Del Prete, 1984; D'Elia et al., 1985; Ishihara and Hsu, 1986). Ishihara and Hsu (1986), show that such instability phenomena occurred as reactivations of quiescent landslides in which residual shear strengths have been mobilized under undrained conditions. The above-mentioned characteristics of many earthquake-induced landslides observed following the 1980 Irpinia earthquake, generated an anomalous spatial distribution of landslides in which the majority of them occurred at large epicentral distances. Del Gaudio and Wasowski (2004) found that in most cases the minimum PGA to trigger reactivated landslides during the 1980 Irpinia earthquake was in the range of 0.05–0.08g, with some of them triggered at PGA values as low as 0.01g.

During the **M**6.1 1997 Umbria-Marche (Central Italy) earthquake, rock falls and rotational slides were the most frequently observed phenomena. Rock falls were widely prevalent (60%) while rotational and translational slides were less frequent (35%). Only a few cases of earth and debris flows have occurred (<5%). Most rock falls have been observed along steep road cuts and they have interested limestones and marly limestones, interbedded by clay and sandstones. The rotational slides occurred in debris deposits and often are the reactivation of pre-existing landslides. The spatial distribution of the triggered landslides highlights that around 60% of landslides occurred within a distance of 10 km from the epicenter and the maximum epicentral distance was 25 km. The **M**6.1 6 April 2009 L'Aquila (Central Italy) earthquake,

triggered a relatively small number of landslides (mainly falls of sedimentary rocks and small debris avalanches). Such phenomena typically occurred at short distance from the epicenter.

3 THE 2016 CENTRAL ITALY SEISMIC SEQUENCE

Between 24 August 2016 and 30 October 2016, a wide region of Central Italy was struck by several earthquakes. Historical seismicity studies (e.g. Rovida et al., 2016) show that this area has been characterized by an intense seismic activity in the past centuries. The first important known earthquake was the **M**5.3 July 1627 Monti della Laga event that was followed by the **M**6.2 7 October 1639 Amatrice earthquake. The latter event caused severe damage in Amatrice and Accumoli. Other events occurred in 1646 (**M**5.9) and in 1672 (**M**5.3). The area was then interested by the catastrophic 1703 January – February seismic sequence, characterized by two main events: **M**6.9 14 January, in the Norcia region, and **M**6.7 2 February in the L'Aquila region. Many additional minor events occurred during the 19th century. More recently, the Central Italy area was interested by the *Ms* 5.9 1979 earthquake, the **M**6.1 1997 Umbria-Marche earthquake, and the **M**6.1 2009 L'Aquila event.

The 2016 seismic sequence was characterized by three mainshocks: (1) **M**6.1 24 August, (2) **M**5.9 26 October, and **M**6.5 30 October. Each event was followed by numerous aftershocks. All mainshocks were caused by normal faults part of the Mt. Vettore-Mt. Bove fault system. The 24 August event caused massive damages especially to the villages of Amatrice, Accumoli, and Arquata del Tronto. In total, there were 299 fatalities, generally from collapses of unreinforced masonry dwellings. The October events caused significant new damage in the villages of Visso, Ussita, and Norcia, although not producing fatalities, since the area had largely been evacuated. The 2016 Central Italy sequence occurred in a gap between two earlier earthquake events, the 1997 **M**6.1 Umbria-Marche earthquake to the north-west and the 2009 **M**6.1 L'Aquila earthquake to the south-east (Stewart et al., 2018; Lanzo et al., 2018).

The **M**6.1 24 August event is a peculiar two-fault event caused by the rupture of the southernmost section of the Mt. Vettore-Mt. Bove fault system and the Amatrice fault in the Laga Mountains. The 26 and 30 October events were both caused by the rupture of the Mt. Vettore - Mt. Bove fault system (Galadini et al., 2018). Comparisons between recorded and predicted ground motions show a relatively good agreement of attenuation with distance of the shaking. As a result, overall, ground motions generated by these events are not unusually strong. However, Zimmaro et al. (2018) show that for many intensity measures, including PGA and PGV, there is a strong attenuation of recorded ground motions with distance.

From a geological point of view, the area is characterized by Miocene flysch units and the Carbonatic units of the Umbria-Marche Succession. Flysch units (Laga formation) consist of alternating sandstone and marls layers, where sandstone is always the prevailing component. The flysch, similar to many other turbidite formations, presents variations in sandstone/marl ratio and layer thickness due to the distance from the source area in the depositional basin. Discontinuity spacing further varies depending on the distance from fault zones. Weathering of marl layers, though limited to extremely shallow depth, occurs soon after marls are exposed from highway cuts and excavations. This weathering is sufficient to undercut overlying sandstone slabs, which can break free when exposed to strong ground motions (GEER, 2017).

4 LANDSLIDES DATA

The 2016 Central Italy seismic sequence has triggered several landslides which occurred in steep slopes and along artificial and natural scarps bordering main and secondary roads. Information about landslides triggered by the three events are mainly based on CERI (2016) and GEER (2016, 2017). We subdivide the landslides inventory into three main categories defined by Keefer (1984): (1) Category I: falls and slides; (2) Category II: coherent slides; (3) Category III: lateral spreads or flow slides. No Category III features have been observed during the 2016 Central Italy earthquake sequence. When observed landslides do not fall into

any of the mentioned standard categories or are not adequately described, they are labelled as "*other*" category. Landslide phenomena observed following the three main events of the seismic sequence are described below.

Figure 1 shows the observed landslides locations and surface fault projections, while Table 1 lists the percentages of observed landslide categories. Most of the observed phenomena (~83%) fall in Category I and involve mainly small rock falls observed along roadways cuts throughout the earthquake zone. Observed Category II landslides are mainly debris slides and rock slide occurring in gentle slope (labelled as "rock slide*"). The distribution of landslides in each category is practically the same for all three events of the 2016 seismic sequence. Such landslide categories distribution is similar to that observed following the 1997 Umbria–Marche earthquake (Esposito et al., 2000).

The landslide phenomena located within the surface fault projection are about 25% of the total for the 24 August and 30 October events. This percentage increases to about 40% for the 26 October event. Figure 2 shows landslide data for the three events compared with the empirical upper bound limits defined by Keefer (1984) in terms of surface-wave magnitude (M_S; assumed to be 6.1 for the 24 August event) versus epicentral distance (R_{epi}; Figure 2a) and Joyner and Boore distance (R_{JB}; Figure 2b).

The same information is reported in planar view in Figure 3 for the 24 August event. Figure 3a and b show landslide locations versus empirical upper bound limits (Keefer, 1984) using R_{epi} and R_{JB} as distance metrics, respectively. The empirical upper-bounds in planar view are drawn in Figure 3 as the loci with the same distance from the epicenter (Figure 3a) or from the surface fault projection (Figure 3b) (dashed lines).

The comparison with the empirical limits shows that the zone involved in the activation of Category I landslides is limited to an area with a radius of about 40 km around the epicenter (about half the distance limit indicated by Keefer (1984) for this kind of phenomena) with the

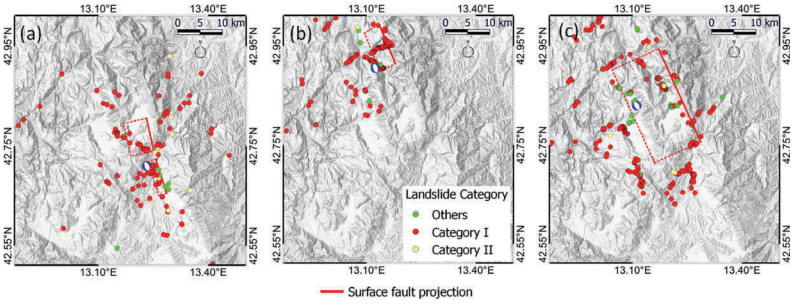

Figure 1. Observed landslides and surface fault projections following the (a) **M**6.1 24 August, (b) **M**5.9 26 October and (c) **M**6.5 30 October 2016 events.

Table 1. Percentage of landslides falling into each category and landslide types for each category.

Event	Category I		Category II		Other
	83%		10%		7%
24	August rock fall	95%	debris slide	71%	
	rock slide	5%	rock slide*	29%	
	90%		5%		5%
26 October	rock fall	94%	debris slide	67%	
	rock slide	6%	rock slide*	33%	
	83%		3%		14%
	rock fall	86%	debris slide	66%	
30 October	rock slide	10%	rock slide*	13%	
	other mech.	4%	earth slide	13%	
			other mech.	8%	

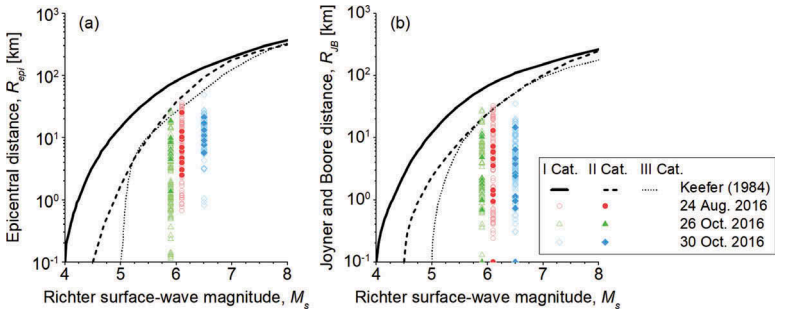

Figure 2. Comparison between (a) epicentral distance and (b) Joyner and Boore distance, for landslides following the three events and the empirical upper-bound curves proposed by Keefer (1984).

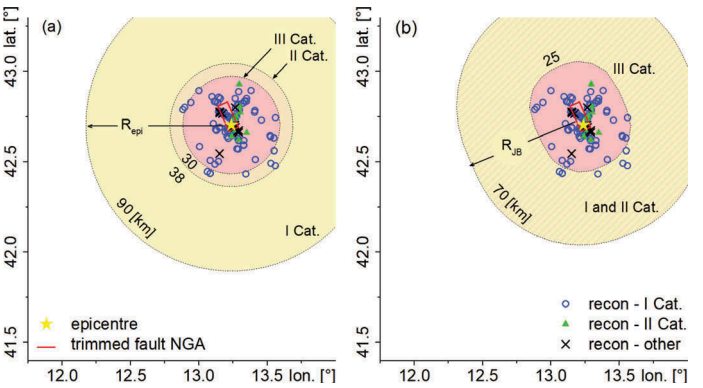

Figure 3. Areal distribution of landslides sites following the 24 August event compared with empirical upper bound loci proposed by Keefer (1984) in terms of (a) epicentral distance and (b) Joyner and Boore distance.

majority being at 10 km or less from the surface ruptures. Comparing all mapped landslides with the Italian landslide inventory (Inventario dei Fenomeni Franosi in Italia, IFFI project, ISPRA – Dipartimento Difesa del Suolo Servizio Geologico d'Italia, available at: http://www.progettoiffi.isprambiente.it), new landslides are mostly in the near-field (< 10 km), while far-field landslides are present in the preexisting landslide inventory (Pavlides et al., 2017).

Figures 4 and 5 show, for the 26 and 30 October events, the areal distribution of landslide sites compared with empirical upper-bound loci defined from Keefer (1984) for epicentral distance (Figures 4a and 5a) and Joyner and Boore distance (Figures 4b and 5b). The comparisons with the empirical limits show that the zones involved in the activation of Category I landslide are limited to an area with a radius of about 30 km and of 40 km around the epicenter for the 26 October event and 30 October event, respectively.

Figure 6 shows the comparison between the envelope area affected by landslides for the three events and the upper bound proposed by Keefer (1984) and Rodriguez et al. (1999). The areas affected by landslides do not increase with the magnitude, as expected from the literature. Figure 7a reports epicentral distance versus magnitude for the three events of the 2016 seismic sequence and the 1997 Umbria–Marche earthquake, used here as a term of comparison. Figure 7b shows the same comparison in terms of Joyner and Boore distance. Landslides triggered by the 2016 seismic sequence have landslides limit distances very similar to those triggered by 1997 Umbria–Marche earthquake.

The spatial distribution of ground motion and the quantification of intensity measures at the outher limit of landsliding (i.e., lower limit at which landslides occur) is an important aspect in the analysis of earthquake-triggered landslides. In this section we show some analysis

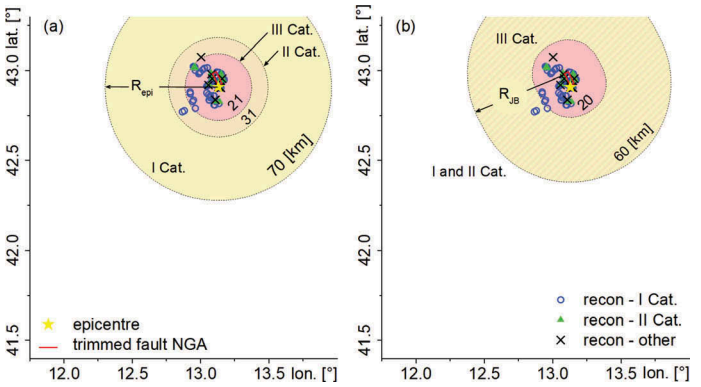

Figure 4. Areal distribution of landslides sites following the 26 October event compared with empirical upper bound loci proposed by Keefer (1984) in terms of (a) epicentral distance and (b) Joyner and Boore distance.

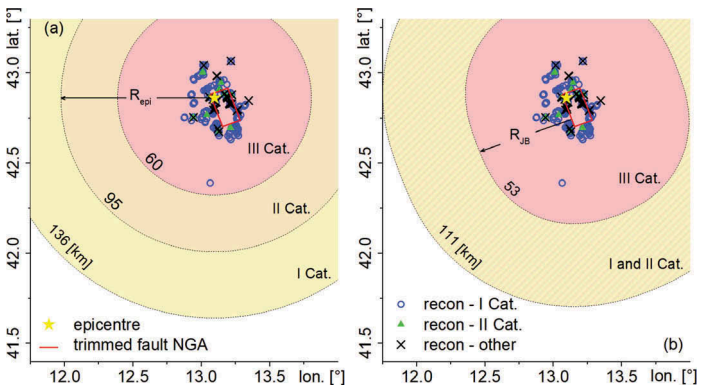

Figure 5. Areal distribution of landslides sites following the 30 October event compared with empirical upper bound loci proposed by Keefer (1984) in terms of (a) epicentral distance and (b) Joyner and Boore distance.

using the peak ground acceleration and velocity (PGA and PGV, respectively) as reference intensity measure. We found that approximately 50% of the reported landslides are observed in the PGA interval of 0.01-0.49 g for the 24 August event, while such range is 0.01-0.38 g and 0.01-0.39 g for the events of 26 and 30 October, respectively. For the 24 August event, landslide limits are observed at eleven locations and the range of PGA values among these limits is 0.02-0.17 g. For the 26 October, PGA values along the landslide limits range from 0.04 to 0.38 g, while for the 30 October, PGA values at landslide limits fall in the range from 0.05 to 0.39 g. The values of PGA at landslide limits are comparable to those observed during other earthquakes of comparable magnitude (Jibson and Harp, 2016). However the lower PGA values are substantially the same for the three events while the upper PGA values of the range are much higher for the October events. This causes an increase in the width range at landslide limits from August event to October events.

Approximately 50% of the reported landslides are observed in the PGV interval 1-39 m/s for the 24 August event, while the range is 1-21 m/s and 1-29 m/s for the 26 October and 30 October events, respectively. For the 24 August event, landslide limits are observed at eleven locations and the range of PGV values among these limits is 3.4-14.2 cm/s. For the 26 October, PGV values along the landslide limits range from 2.4 to 23.9 cm/s, while for the 30 October, PGV values at landslide limits fall in the range from 7.7 to 39.8 cm/s.

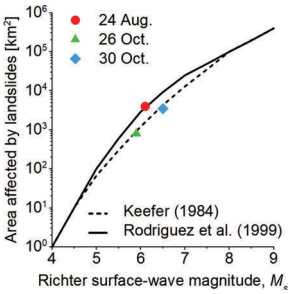

Figure 6. Comparison between the envelope area affected by landslides and the upper bound proposed by Keefer (1984) and Rodriguez et al. (1999) for the three events.

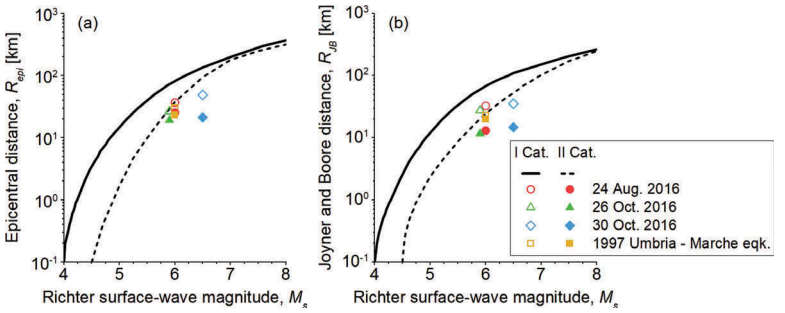

Figure 7. Comparison between the three events of the 2016 seismic sequence and those of landslides triggered by the 1997 Umbria – Marche earthquake in terms of (a) epicentral distance (b) Joyner and Boore distance, for landslides Category I and Category II.

5 CONCLUSIONS

Assessing the spatial distribution of landslides triggered by an earthquake (or earthquake sequence) is not only important in understanding physical phenomena, but also to establish hazard zoning in seismic active areas. In this paper, we describe landslide spatial distributions and types of instability phenomena triggered by three major events during the 2016 Central Italy seismic sequence. We show that landslides limit distances from the analyzed sequence are in good agreement with empirical upper-bound curves proposed in the literature. Our comparisons are performed both in terms of epicentral and and Joyner and Boore distances. We also compare such limit distances with landslides triggered by the 1997 Umbria–Marche earthquake, showing similar outcomes

Remarkably, the areas affected by earthquake-induced landslides do not increase with magnitude for the three mainshocks of the 2016 Central Italy seismic sequence. This is somewhat unexpected if looking at the existing literature. Threshold PGA and PGV values at the outer limit of the landslides, highlight different behaviors following the three mainshocks. The width range of PGA and PGV at landslide limits is larger for the October events.

REFERENCES

Ambraseys, N.N. 1976. The Gemona di Friuli Earthquake of 6 May 1976, *UNESCO Restricted Tecnical Report* RP/1975-76/2.222.3, Part II.

CERI working group: Martino, S., Caporossi, P., Della Seta, M., Esposito, C., Fantini, A., Fiorucci, M., Iannucci, R., Marmoni, G.M., Mazzanti, P., Missoni, C., Moretto, S., Rivellino, S., Romeo, R.W., Sarandrea, P., Troiani, F., Varone, C. 2016. *Sisma Centro Italia: Amatrice, Visso, Norcia Effetti- Interazione rete infrastrutturale*. Available at http://www.ceri.uniroma1.it/, last accessed April 19, 2018.

Cotecchia, V. and Del Prete, M. 1984. The Reactivation of Large Flows in the Parts of Southern Italy Affected by the Earthquake of November 1980, with Reference to the Evolutive Mechanism, *Proceedings of the Fourth International Symposium on Landslides, Toronto*, 2: 33–37.

D'Elia, B., Esu, F., Pellegrino, A., and Pescatore, T. 1985. Some Effects on Natural Slope Stability Induced by the 1980 Italian Earthquake. *Proceedings of the Eleventh International Society of Soil Mechanics and Foundation Engineering Conference, San Francisco*.

Del Gaudio, V., and Wasowski, J. 2004. Time probabilistic evaluation of seismically-induced landslide hazard in Irpinia (southern Italy). *Soil Dynam. Earthq. Eng*. 24: 915–928.

Esposito, E., Gargiulo, A., Iaccarino, G. and Porfido, S. 1998. Distribuzione dei fenomeni franosi riattivati dai terremoti dell'Appennino Meridionale. Censimento delle frane del terremoto del 1980. *Proc. Int. Conf. Prevention of hydrogeological hazards, Italy*, 1: 409-429. In Italian.

Esposito, E., Porfido, S., Simonelli, A.L., Mastrolorenzo, G., Iaccarino, G. 2000. Landslides and other surface effects induced by the 1997 Umbria–Marche seismic sequence. *Engineering Geology* 58: 353–376.

Franke K.W., Lingwall B.N., Zimmaro P., Kayen R.E., Tommasi P., Chiabrando F., Santo A. (2018). A Phased Reconnaissance Approach to Documenting Landslides Following the 2016 Central Italy Earthquakes. *Earthquake Spectra* 34: 1693–1719.

Galadini F., Falcucci E., Gori S., Zimmaro P., Cheloni D., and Stewart J.P. 2018. Active faulting in source region of 2016–2017 Central Italy event sequence. *Earthquake Spectra* 34: 1557–1583.

GEER 2016. Engineering Reconnaissance of the 24 August 2016 Central Italy Earthquake. Version 2, Zimmaro P. and Stewart J.P. editors, *GEER Association Report No. GEER-050B*. DOI: 10.18118/G61S3Z.

GEER 2017. *Engineering Reconnaissance following the October 2016 Central Italy Earthquakes. Version 2*, Zimmaro P. and Stewart J.P. editors, *GEER Association Report No*. GEER-050D. DOI: 10.18118/G6HS39.

Govi, M. 1977. Photo-interpretation and Mapping of the Landslides Triggered by the Friuli Earthquake (1976), *International Association of Engineering Geology Bulletin* 15: 67–72.

Ishihara, K. and Hsu, H.L. 1986. Considerations for landslides in natural slopes triggered by earthquakes. *Proc. of Japanese Society of Civil Engineers (JSCE) 376/III-6* (Geotechnical Engineering).

Jibson, R.W. and Harp, E. L. 2016. Ground Motions at the Outermost Limits of Seismically Triggered Landslides. *Bulletin of the Seismological Society of America* 106: 708–719.

Keefer, D.K. 1984. Landslides caused by earthquakes, *Geol. Soc. Am. Bull*. 95: 406–421.

Lanzo, G., Tommasi, P., Ausilio, E., Aversa, S., Bozzoni, F., Cairo, R., d'Onofrio, A., Durante, M.G., Foti, S., Giallini, S., Mucciacciaro, M., Pagliaroli, A., Sica, S., Silvestri, F., Vessia, G., and Zimmaro, P. 2018. Reconnaissance of geotechnical aspects of the 2016 Central Italy earthquakes. *Bulletin of Earthquake Engineering*. DOI: 10.1007/s10518-018-0350-8.

Pavlides, S., Chatzipetros, A., Papathanasiou, G., Georgiadis, G., Sboras, S., and Valkaniotis, S. 2017. Ground deformation and fault modeling of the 2016 sequence (24 Aug.–30 Oct.) in central Apennines (Central Italy). *Bulletin of the Geological Society of Greece* 51: 76–112.

Rodríguez, C.E., Bommer, J.J., and Chandler R.J. 1999. Earthquake-induced landslides: 1980–1997, *Soil Dynam. Earthq. Eng*. 18: 325–346.

Romeo, S., Di Matteo, L., Melelli, L., Cencetti, C., Dragoni, W., and Fredduzzi, A. 2017. Seismic induced rockfalls and landslide dam following the October 30, 2016 earthquake in Central Italy. *Landslides* 14: 1457–1465.

Rovida A., Locati, M., Camassi, R., Lolli, B., and Gasperini, P. (Eds.) 2016. CPTI15, the 2015 version of the Parametric Catalogue of Italian Earthquakes. *Istituto Nazionale di Geofisica e Vulcanologia*, DOI:10.6092/INGV.IT-CPTI15.

Silvestri, F., Forte, G., and Calvello, M. 2016. Multi-level approach for zonation of seismic slope stability: Experiences and perspectives in Italy. *Panel report. 12th International Symposium on Landslides, Napoli (Italy)*, 12-19 June 2016 'Landslides and Engineered Slopes. Experience, Theory and Practice' (Eds: Picarelli L., Scavia C., Aversa S., Cascini L.), 1: 101-118. London: Taylor and Francis Inc., ISBN: 978-113802988-0.

Stewart, J.P., Zimmaro, P., Lanzo, G., Mazzoni, S., Ausilio, E., Aversa, S., Bozzoni, F., Cairo, R., Capatti, M.C., Castiglia, M., Chiabrando, F., Chiaradonna, A., d'Onofrio, A., Dashti, S., De Risi, R., de Silva, F., della Pasqua, F., Dezi, F., Di Domenica, A., Di Sarno, L., Durante, M.G., Falcucci, E., Foti, S., Franke, K.W., Galadini, F., Giallini, S., Gori, S., Kayen, R.E., Kishida, T., Lingua, A., Lingwall, B., Mucciacciaro, M., Pagliaroli, A., Passeri, F., Pelekis, P., Pizzi, A., Reimschiissel, B., Santo, A., Santucci de Magistris, F., Scasserra, G., Sextos, A., Sica, S., Silvestri, F., Simonelli, A.L., Spanò, A., Tommasi, P., and Tropeano, G. 2018. Reconnaissance of 2016 Central Italy Earthquake Sequence. *Earthquake Spectra* 34: 1547–1555.

Zimmaro, P., Scasserra, G., Stewart, J.P., Kishida, T., Tropeano, G., Castiglia, M., and Pelekis, P. 2018. Strong ground motion characteristics from 2016 Central Italy earthquake sequence. *Earthquake Spectra* 34: 1611–1637.